South African Journal of Chemical Engineering 29 (2019) 17–23

Contents lists available at ScienceDirect

South African Journal of Chemical Engineering

journal homepage: www.elsevier.com/locate/sajce

Toxicology evaluation and antidermatophytic activity of silver nanoparticles synthesized using leaf extract of *Passiflora caerulea*

J. Santhoshkumar[a], B. Sowmya[a], S. Venkat Kumar[a], S. Rajeshkumar[b,*]

[a] School of Bio-Sciences and Technology, Vellore Institute of Technology (VIT), Vellore, 632014, TN, India
[b] Department of Pharmacology, Saveetha Dental College and Hospitals, Saveetha University, SIMATS, Chennai, 600077, TN, India

ARTICLE INFO

Keywords:
Antidermatophytic activity
Nanotoxicity
Embryonic toxicity
Passiflora caerulea

ABSTRACT

Current report in this study, using plant-derived nanoparticles and green synthesis has become the emerging area of research. It was originated to enhance our insight on the strength and environment impact of silver nanoparticles (Ag-NP). The particles were synthesized using *Passiflora caerulea* leaf extract and characterized by using UV-visible, XRD, TEM, SEM, EDAX, FTIR, AFM analysis. The silver nanoparticles (AgNPs) are known to be one of the most versatile inorganic nanoparticles with its application in the treatment of human pathogens, and we focused the nanoparticles toxicity. In the result, we found a maximum zone of inhibition *Trichophyton rubrum* 104.648 ± 0.008 when compared with the control. The mean standard deviation for the silver nanoparticles which was available for the size was nearly 23.94 ± 8.67 nm. Besides, the toxicity was life stage dependent. The zebrafish embryos/larvae are additionally mentioned lethal concentration of silver nanoparticles 80 µg/ml and instructed during this study as a good protocol for evaluating the potential toxicity of nanoparticles.

1. Introduction

Nanotechnology is an emerging field of modern research which deals with the synthesis of particle's structure measuring from approximately 1 to 100 nm in size. Within this size range all the properties (chemical, physical and biological) changes in fundamental ways of both individual atoms/molecules and their corresponding bulkiness of nanoparticles they form. The applications of nanoparticles and nanomaterials are proliferating on various fronts due to their enhanced properties based on the size, bio-distribution, and morphology (Rajeshkumar et al., 2015).

Nanobiotechnology is a novel tool that improves the technique to target common plant fungal diseases. The Phyto-mediated synthesis is a suitable and most acceptable biosynthetic method for synthesis of metal nanoparticles. Recently, various plant parts like bark, leaf, fruit, stem and seed extracts have been successfully used for the synthesis of metal nanoparticles (Mittal et al., 2013), (Mittal et al., 2013). Among different metal nanoparticles, silver (Ag) nanoparticles have been used extensively due to their potential anti-bacterial (Mohanta et al., 2016). Anti-fungal and anti-proliferative activity (Nayak et al., 2015). Due to the excellent antimicrobial properties, the silver (Ag) nanoparticles have been used in food packaging, seed preservation, bio fertilisers, cosmetics and medicine (Dipankar and Murugan, 2012). The applications of silver nanoparticles were also found to be implemented widely in the field of high sensitive biomolecular detection, diagnostics, catalysis, and microelectronics (Mohanta and Behera, 2014). Also, the utilization of little mammalian models for substantial scale screening for poisonous quality and bioavailability might be less financially doable (Ali et al., 2019). It has also been acknowledged to have strong inhibitory and anti-fungal along with bactericidal effects, anti-inflammatory and anti-angiogenesis activities (Abourashed et al., 2002). Silver nanoparticles have gained great interests due to their unique properties such as chemical stability, catalytic and excellent conductivity. It can be incorporated into composite fibres, cryogenic superconducting materials, cosmetic products, food industry and electronic components (Magudapathy et al., 2001). In biomedical applications; it has been added to wound dressings, topical creams, antiseptic sprays and fabrics, as an antiseptic and displays a broad biocidal effect against microorganisms through the disruption of their unicellular membrane thus, disturbing their enzymatic activities (Klaus-Joerger et al., 2001), (Syed and Ahmad, 2012). Silver nanoparticles provide better efficacy for the control of plant diseases and damage caused by some fungal strains, which lead to pathogenic effects in human for example mushrooms (Kim et al., 2012), (Berger et al., 1976). The possible benefits of employing nanobiotechnology to agriculture, it is necessary to study the antifungal activity of silver nanoparticles

* Corresponding author. Department of Pharmacology, Saveetha Dental College and Hospitals, Saveetha Institute of Medical and Technical Sciences (SIMATS), Chennai, 600077, TN, India.
E-mail address: ssrajeshkumar@hotmail.com (S. Rajeshkumar).

https://doi.org/10.1016/j.sajce.2019.04.001
Received 5 March 2019; Received in revised form 9 April 2019; Accepted 17 April 2019

against antidermatophytic activity (Mohanta et al., 2016). Then again, Ag NP may cause themselves an unfavourable impact on life framework because of specific properties of AgNPs or a consolidated instrument of poisonous quality because of the nearness of both Ag^+ particles and AgNP may happen (Kaba and Egorova, 2015; Abramenko et al., 2018).

P.caerulea is considered valuable to have herbal activity as a sedative and anticonvulsant, the treatment of the manic phase of bipolar disorder, the symptoms associated with neuralgia and shingles, the fretfulness of teething children, and other general pain also used to treat tension-related asthma, and as an anxiolytic, muscle relaxant, antidepressant, and as an adaptogen (Abourashed et al., 2003). In current scenario number of studies investigating the toxicity of AgNP, in a range of fish species, have provided evidence for concentration-dependent toxicity (Van Aerle et al., 2013). A reasonable comprehension of how extraordinary qualities of nanoparticles contribute to their dangerous conduct to living beings are essential for anticipating and control nanotoxicity (Sarkar et al., 2018). Based on these realities, zebrafish embryos are appropriate in vitro model for assessing the toxicity of nanomaterials (Mosselhy et al., 2016).

2. Material and methods

2.1. Materials

Silver nitrate ($AgNO_3$) as a precursor was purchased from Sigma-Aldrich. All other reagents were of analytical grade. Ultra-pure (Milli-Q) water was used throughout the whole experiment. Mueller Hinton agar (MHA) was used for the cultivation of fungi, which was obtained from Hi-media laboratories, Mumbai, India. Standard fungal strains of clinical significance such as *Trichophytonmenta grophytes* MTCC 7687, *Trichophytonrubrum* MTCC 7859, *Epidermophyton floccosum* MTCC 7880, *Microsporum audouinii* MTCC 8197, *Microsporum Canis* MTCC 3270 were obtained from Microbial Type Culture Collection (MTTC), Chandigarh.

2.2. Plant collection

The fresh leaves of P. *caerulea*L. (Passifloraceae) Were collected in sterile polythene bag from the garden of VIT University Vellore, few amounts of leaves were taken for research purpose, and remaining were preserved in the refrigerator for future use. The leaves were washed with tap water to remove all the dust and then double washed with de-ionized water.

2.3. Preparation of the plant extract

5 g of fresh leaf sample was weighed and soaked in double distilled water then the chopped leaves were subjected to boiling at 70 °C for 8 min, an extract was collected by simple filtration using Whatman filter paper 42, and the extract was stored at a low temperature until there was no further use.

2.4. Biosynthesis of silver nanoparticles and characterization

The synthesis of silver nanoparticles using plant extract 0.01 M of Silver Nitrate ($AgNo_3$) was dissolved in 90 ml of Milli-Q water, and then 10 ml of the leaves extract was added to it. The solution was kept in the stirrer for 20min. A yellow colour solution had appeared after the incubation time, and that confirmed the synthesis of AgNPs. The biosynthesis of the silver nanoparticles in aqueous solution was monitored periodically in UV-Vis spectrophotometer within the range of 200–500 nm. The average size and surface charge of the AgNPs were analysed by Zeta sizer. The particle diameters were assessed at a scattering angle of 90°at room temperature (25 °C). Fourier Transform Infra-Red spectra of the AgNPs were studied in FT-IR spectrophotometer in transmission mode with 200 scans. The size of the silver nanoparticles was confirmed by analysis of morphological structure under a scanning electron microscope (SEM) and Transmission electron microscope (TEM). The topography of the nanoparticles was characterized using Atomic Force Microscopy (AFM). Elemental compositions of the synthesized nanoparticle were described using Elemental Dispersion Analysis of X-ray. XRD diffraction pattern was recorded for silver nanoparticles to examine the crystalline structure.

2.5. Zebrafish embryotoxicity (mortality and hatchability rate)

Exposures were led per OECD rule 236 with slight variation (Guidelines et al., 2013). Briefly, viable zebrafish embryos (< half dozen hpf) were used, and healthy impregnated embryos at similar organic process stage were collected for exposures. Fruitless or unfortunate incipient organisms alluded to as white and dark were disposed of. Exposures were initiated by concisely transferring embryos to a petri-dish containing a fresh medium, for controls or exposure answer. After, the embryos were transported separately to wells of U-bottom 24-well plates and incubated for 96 h in five cubic centimetre answer. The tested concentrations for every of the 2 Cu forms were ten, 20, 40, 60 and eighty μg/L Silver Nanoparticles. All through the introduction day, perceptions were led to evaluate mortality and bring forth. Embryo mortality was recorded when 24, 48, 72 and 96 h incubation. Mortality was expressed as the proportion of dead embryos at any time purpose. Hatching success was shown as the proportion of hatched embryos when 96 h. The check was disbursed with their replicates; every consisting of eight separately exposed embryos or 16 for controls.

3. Results and discussion

3.1. UV-Visible spectroscopy study

UV spectroscopy is a technique used to determine the formation and stability of metal nanoparticles at different duration (1 hr to 6 hrs), shown in (Fig. 1) and also the reduction of Ag^+ ions to Ag^0 by Passiflora caerulea leaf extract was observed. By adding the different concentration of silver ions, the reaction mixture changes the colour. This is on account of the excitation of surface plasmon reverberation in silver nanoparticles (K and J, 2017). Due to the free conduction electrons induced by electromagnetic field, the SPR accepts the dark brown colour of silver colloids, and the conducting particles oscillate at a particular wavelength because of SPR (Santhoshkumar et al., 2017). The P. *caerulea* L. leaf extract was added to 0.01 M silver nitrate resolution, that resulted in an exceedingly colour modification of resolution from yellow to dark brown. The UV-visible spectrometry analysis, spectrum analysis, spectrographic analysis, chemical analysis and qualitative analysis of nanoparticles fashioned within the reaction mixture has an absorption peak close to at 379 nm, that is explained because of the impact of surface plasmon resonance (SPR) of

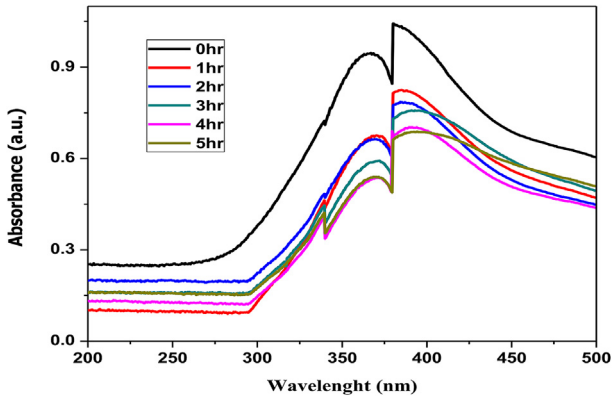

Fig. 1. UV-Vis spectra of the synthesized silver nanoparticles from P. *caerulea* L. extract.

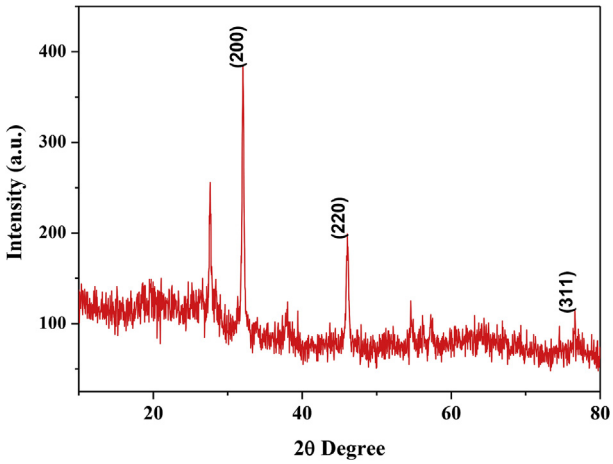

Fig. 2. XRD diffractogram of silver nanoparticle synthesized by P. *caerulea* L. extract.

nanoparticles. The peak shift to 379 nm is revealed due to the excitation of the free electrons by the phytochemicals present in the P. *caerulea* L. extract (Govindarajan et al., 2016).

3.2. X-ray diffraction

The stage purity and crystalline nature conformation of AgNPs was examined by XRD as shown in (Fig. 2). The XRD spectra compared with the quality information that the silver metal shaped in our experiments were within the kind of face centred cubical crystalline lattice as confirmed by AgNPs, which showed three distinct diffractions 2θ peak at 32.0°,46.0°,77.2° corresponding to (2 0 0), (2 2 0), (3 1 1) respectively. The sharp and intense peaks from the XRD patterns reveal the formation of the excellent crystalline part that exists within the compounds. And it is matched with standard JCPDS data card no: 89-3722. Which is reported with previous work (M. Awwad et al., 2013). According to the peak at 32°, the crystallization of reducing and capping agents occurred on the surface of the silver nanoparticles (Kanmani and Lim, 2013).

The average particle size was calculated from Debye-Scherrer formula,

$$D = \frac{0.9\lambda}{\beta\cos\theta}$$

Where λ is the X-ray wavelength, β is the full width half maximum intensity value, and θ is the Bragg's angle. The average particle size was calculated as 15.95 nm. Using the XRD data the lattice parameter and various structural parameters such as crystallite size, dislocation density, lattice strain, the surface area also were calculated which are shown in Table 1.

3.3. FT-IR analysis of silver nanoparticles

The potential biomolecules identify from FTIR spectral measurements were carried out in P. *caerulea*L. The extract which is responsible for reducing and capping the reduced silver nanoparticles. The FTIR spectra are represented in the (Fig. 3), the peaks of synthesized AgNPs synthesized using P. *caerulea*L. FTIR peak noticed at 1236.4, 1369.5, 1635.6 and 3319.1 cm^{-1} in the spectrum. The distinctive peak observed in biomolecule compounds shows peaks for C-N amine group, O-H phenol, C = C Alkenes, N-H amine groups. The plant compound and silver nanoparticles similarly correlated from 1213.23 to 1236.4, 1367.53–1369.5, 1635.6–1635.64, 3304.06–3319.1 cm^{-1} (Mohanta et al., 2016). This clearly shows that the oxidised phenols and polyphenols have capped the surface of the AgNPs (Dipankar and Murugan, 2012).

3.4. Scanning electron microscope analysis of silver nanoparticles

The SEM image of the AgNPs synthesized from the P. *caerulea L.* leaf extract is shown in (Fig. 4). SEM has provided the perspective of the morphology and size of the synthesized silver nanoparticles, which revealed small aggregate triangle and spherically shaped particles. The aggregated particles formation may be due to the existence of phytochemicals present in the leaf extract. The average particles size measured from SEM images is around 100–300 nm (Govindarajan et al., 2016).

3.5. EDX analysis

Energy dispersive X-ray spectroscopy (EDX) is an analytical technique used for the elemental analysis and finds the percentage of chemical composition for the existing of a sample. It is also useful to identify the formation compounds, and their relative proportions in the current mixtures (Fig. 5). EDX spectra confirmed the presence of AgNPs as confirmed by robust signal energy peaks for silver atoms within the variation of 3 keV (Amichai and Grunwald, 1998). Oxygen, chloride and other single elements are also detected which is due to surface plasmon resonance detected in 45.5% of Ag (Magudapathy et al., 2001).

3.6. AFM analysis

AFM defined Silver nanoparticles for its size and surface topography in the non-contact mode with Si element cantilevers with force constant 0.03–0.76 N m-1, Tip height 10–15 μm. It also displays the image in 2-Dimension and 3-Dimension as shown in (Fig. 6). The primary technique was to observe the AgNPs dissolution and agglomeration pattern. The topography of AFM micrography clearly indicates that formulated AgNPs possess spherical shape and size with white patches. It shows that the particles size is larger and additionally the scale value is greater than TEM measurements. The form of the tip AFM could cause da ishonorable crosswise read of the sample. So, the width of the nanoparticles depends on probe shape (Alahmad et al., 2013). The irregular surface morphology was due to the presence of each individual and agglomerative AgNPs.

3.7. TEM analysis

The high-resolution studies with morphological structure and distribution of synthesized silver nanoparticles characterized at higher magnifications (10 nm) were done by TEM as shown in (Fig. 7 A). The result exhibits that the majority of the particles were spherical with smooth surface crystalline nature. The (Fig. 7 B) shows the selected area electron diffraction (SAED), based on particles size distribution; the peaks were plotted in the form of a number frequency histogram of particle size data in linear scale. As it is detected in (Fig. 7 C), the size

Table 1
Structural Parameters of silver nanoparticle synthesized by P. *caerulea* L. extract.

Sample	Lattice parameter	Volume (m^3)	Particle size(D) (nm)	Lattice Strain (ε) (10^{-3})	Dislocation density (δ) (lines/cm^2) (10^{15})	Surface area (S) m^2/g
AgNPS by *P.caeruleaL.extract*	4.2016 ± 0.003	74.17	15.95	1.15	1.26	62.03

Table 2
Minimum inhibitory concentration of the standard drug and antidermatophytic activity of silver nanoparticles.

Sl. No.	Pathogens	Zone of Inhibition (in mm) for AgNP's				Zone of inhibition (in mm) for standard drugs		
		5 µg	25 µg	50 µg	75 µg	Fluconazole	Amphotericin B	Ketoconazole
1	*Tricophyton metagrophytes* **7687**	-	58.42 ± 0.007	67.31 ± 0.004	83.566 ± 0.009	66.548 ± 0.009	79.502 ± 0.010	52.324 ± 0.004
2	*Tricophyton rubrum* **7859**	-	68.326 ± 0.006	69.04 ± 0.012	104.648 ± 0.008	101.346 ± 0.013	76.454 ± 0.010	110.998 ± 0.016
3	*Epidermophyton floccosum* **7880**	20.066 ± 0.002	69.85 ± 0.005	72.898 ± 0.004	75.946 ± 0.009	73.152 ± 0.008	83.566 ± 0.014	67.056 ± 0.006
4	*Microsporum audouinii* **8197**	10.001 ± 0.004	55.626 ± 0.007	75.184 ± 0.002	99.314 ± 0.015	41.148 ± 0.010	76.454 ± 0.006	58.928 ± 0.004
5	*Microsporum canis* **3270**	-	-	-	66.04 ± 0.003	-	58.674 ± 0.006	-

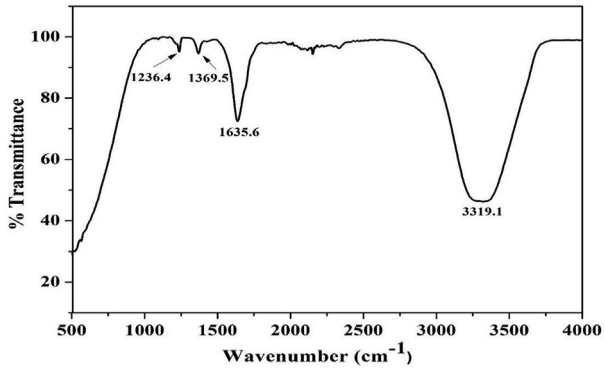

Fig. 3. FTIR Spectrum of silver nanoparticle synthesized by P. *caerulea* L. extract.

distribution of particles toward the tip of the particles size scale is that the majority of the important powder sample once premediated the linear range. The average particles size of silver nanoparticles synthesized using P. *caerulea* L. leaf extract is respect to the mean diameter and variance of silver nanoparticles is 23.94 ± 8.67 nm (K and J, 2017).

3.8. The antidermatophytic activity of synthesized AgNPs

The Dermatophytes activity of the synthesized AgNPs was performed by an agar disc diffusion method using Muller Hinton agar against fungal pathogens (Table 2). *T. mentagrophytes*, *T. rubrum, E. floccosum, M. audouinii, M. Canis*. The spores of each fungal species were suspended into a test tube containing 10 ml of sterile distilled water. The concentration of 5 µL, 25 µL, 50 µL and 75 µL of AgNPs solution was added to the well and incubated for 24 h at 37 °C. Commercial antibiotic discs were placed along with control. After the incubation period, different concentration levels of a zone formed were measured. In the current study, amphotericin B, fluconazole and ketoconazole were used as a positive control toward fungi; amphotericin B is a fungicidal agent widely used in treating serious systemic infections, fluconazole is used in the treatment of superficial skin infections caused by dermatophytes, Candida species and ketoconazole used for the treatment of local and systemic fungal infection (Amichai and Grunwald, 1998).

Trichophyton species play a significant role in dermatophyte infections of each foot and skin. In North America, *T. rubrum and T. mentagrophytes* square measure the foremost frequent pathogens related to onychomycosis (Mousavi et al., 2015). This study was performed to investigate the synthesized silver nanoparticles using *P. caerulea* against dermatophytes infection caused by *M. Canis* 3270, *M. audouinii* 8197, *T. mentagrophytes* 7687, *T. rubrum* 7859 and *E. floccosum*. Our result discloses antifungal activity to AgNPs with the following order of resistance: *T. rubrum* > *M. audouinii* > *T. mentagrophytes* > *E. floccosum* > *M. canis*. The ability of AgNPs inhibition of fungal clearly demonstrated that the zone of inhibition (mm) gradually increased as the concentration of the AgNPs increases, in which *T. rubrum* shows 104.648 ± 0.008 than fluconazole 101.346 ± 0.013, *M. audouinii* 99.314 ± 0.015 greater than Amphotericin B 76.454 ± 0.006, *T. mentagrophytes* 83.566 ± 0.009 greater than Amphotericin B 79.502 ± 0.010 (Table 1). Whereas, the previous data indicates that the AgNPs had good antifungal and antimicrobial activity (Rajeshkumar and Kayalvizhi, 2015). Reported the expansion inhibition of the AgNPs on T. mentagrophytes and C. albicans were 4 ± 2.0 mg/mL-1 and 5 ± 0.10 mg/mL-1, severally (Bhalodia and Shukla, 2011). Showed that AgNPs had an inhibitory effect on the growth of *T. mentagrophytes*, *T. rubrum* AgNPs (IC80, 1–7 mg. mL-1) exhibited greater efficacy than fluconazole (IC80: 10–30 mg. mL-1), but less active than Amphotericin B (IC80: 15 g.mL-1). Though *E. floccosum* gives 75.946 ± 0.009 which is greater than *M. canis* 66.04 ± 0.003. The

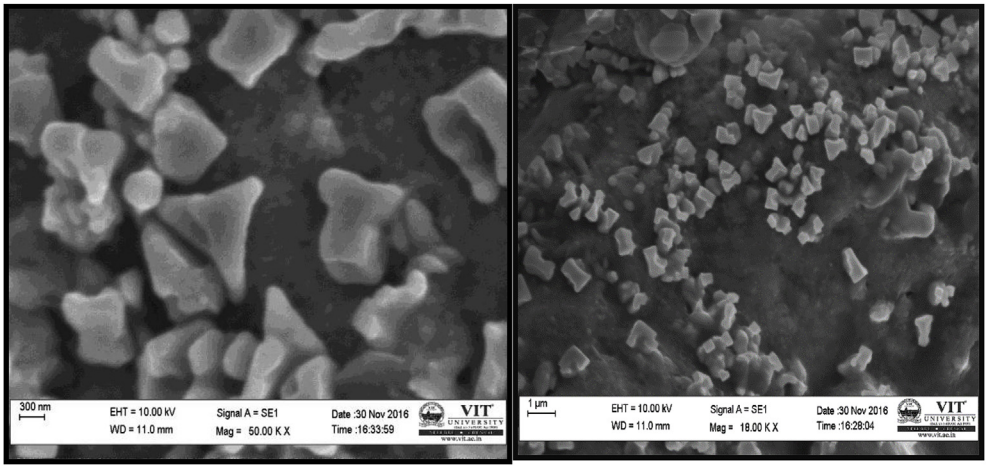

Fig. 4. Surface morphology of silver nanoparticle synthesized by P. *caerulea* L. extract.

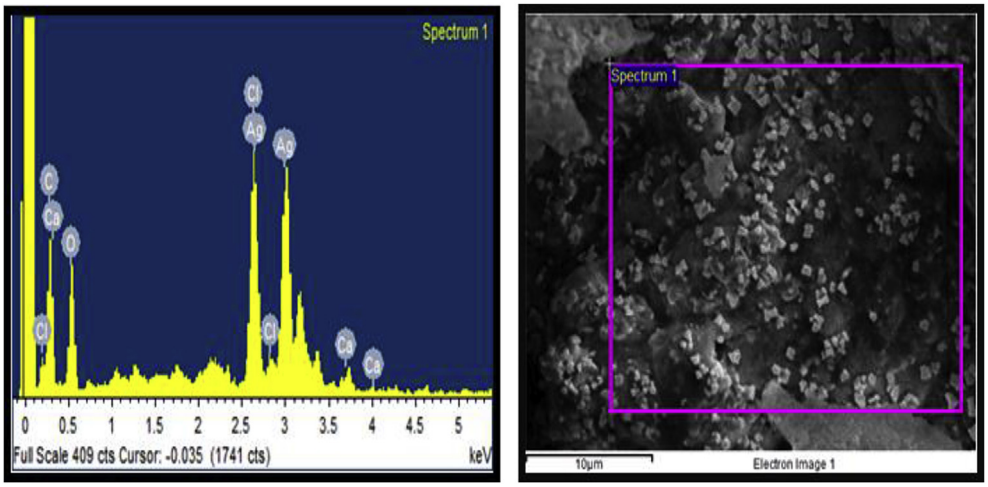

Fig. 5. EDX spectrum of synthesized silver Nanoparticles by P. *caerulea* L. extract shows 45.50 wt per cent of Ag metal in the sample.

above results show the hopeful antifungal activity of silver nanoparticles against dermatophytes. Hence, forth the upcoming work has to be focused on its medicinal applications (Singh and Vidyasagar, 2014).

3.9. Toxicology analysis using zebrafish study

The hatching rates were significantly decreased in *Myristica fragrans* mediated synthesized silver nanoparticles (86 µg/ml) exposed groups compared to the control (Fig. 8). Percentage of hatched embryos, determined from the proportion of embryos that survived to 72 hpf (mean numbers of surviving embryos that hatch: control, 18/21; 1–10 hpf, 8/12; 10-72 hpf, 12/14; 1–72 hpf, 1/4). Data are means ± S.E.M., (n = 30). The control and each treatment were conducted in triplicated test vessels, with each beaker consisting of 30 embryos.

Cumulative mortality of zebrafish embryos exposed to silver nanoparticles at low concentration or with 40 µg/ml ppt and high concentration of 120 µg/ml open circles at 16 hpf. Data are means ± S.E.M., n = 6 independent samples per treatment. Mortality of embryos in silver nanoparticle exposing conditions was between 25 and 36% in all beakers, and there was not much effect of silver nanoparticles exposure conditions on embryo mortality (Fig. 9). There were not many clear indications of abnormal development or morphology of embryos at the end of the exposure period (96 hpf). As a result, nanotoxicity research is deriving attention. The size of the particles used in this study was about 4–10 nm. Hence, the toxicity profiles obtained on silver nanoparticles of these sizes only moreover the particles are more significant in size could be different than the one observed here (Bar-Ilan et al., 2009). In this study, zebrafish embryos were treated with AgNPs (40, 60, 80 and 120 µg/ml) during 4–96 hpf. A concentration-dependent increase in mortality and hatching delay was determined in AgNPs treated embryos for 20 ppt/ml in virtually 90th cases. Notably, the Ag nanoparticles induce distinctive stage and dose-dependent phenotypes and nanotoxicity, upon their acute exposure to the AgNPs significantly for 20 ppt/ml on the far side 96 hpf. Similar studies are in going to examine the toxicity of Ag nanoparticles in rats and another vertebrate model system (Krishnamurthy et al., 2009).

4. Conclusion

Silver nanoparticles (AgNPs) were successfully obtained from bioreduction of silver nitrate solutions using *P. caerulea* leaf extracts. Owing to varying properties of these species, AgNPs obtained from them also varied in size of the 10 nm and spherical shape. AgNPs have been appropriately characterized using UV-vis spectroscopy, SEM, TEM and EDS, AFM, XRD analysis. Silver NPs were successfully biosynthesized by this simple, fast, cost-effective, eco-friendly, and efficient method,

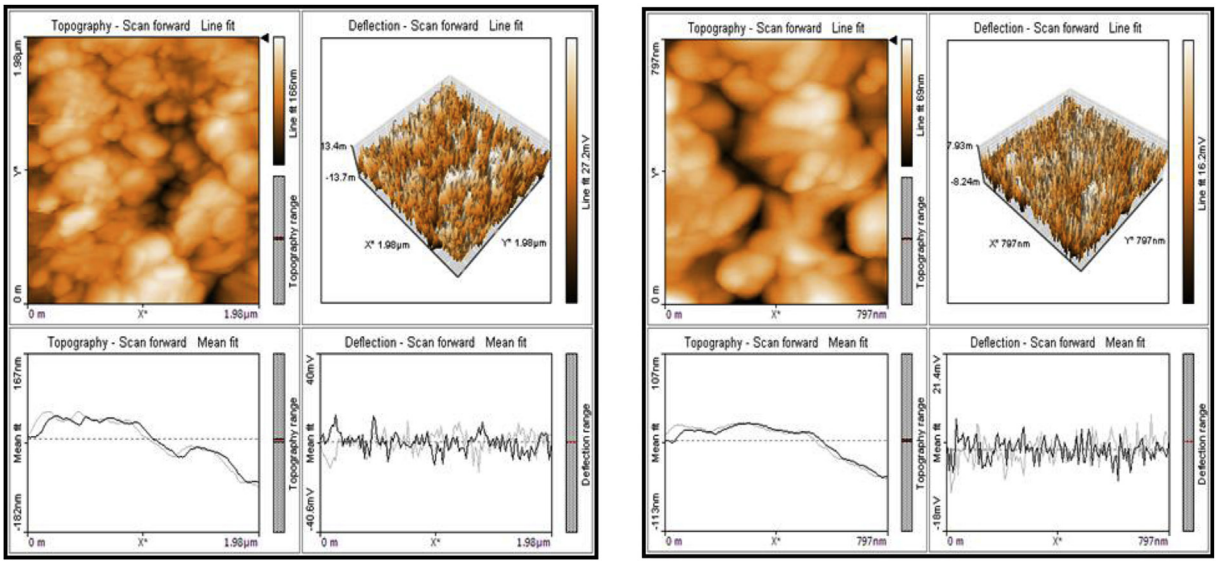

Fig. 6. AFM pictographs of silver nanoparticles synthesized by P. *caerulea* L. extract.

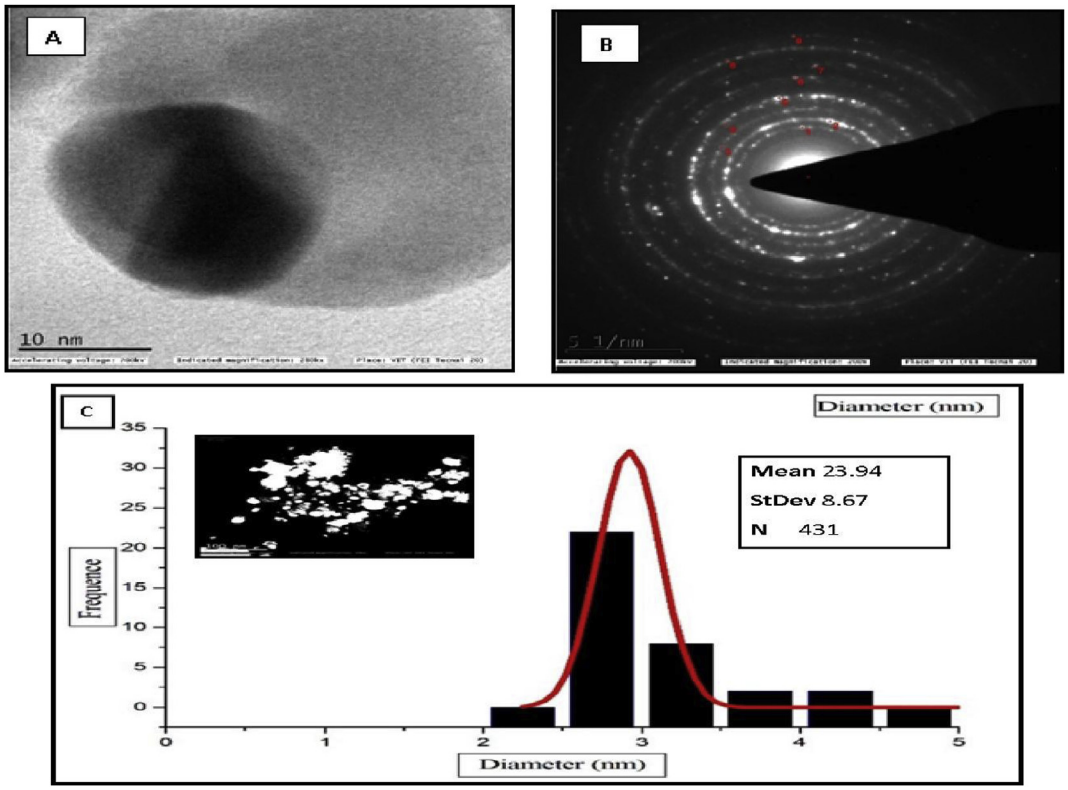

Fig. 7. (A). A TEM image of synthesized nanoparticles from plant extract (scale bars correspond to 10 nm) (B). Selected area of electron diffraction pattern recorded from one of the silver nanoparticles (C). Particle size distribution of silver nanoparticles.

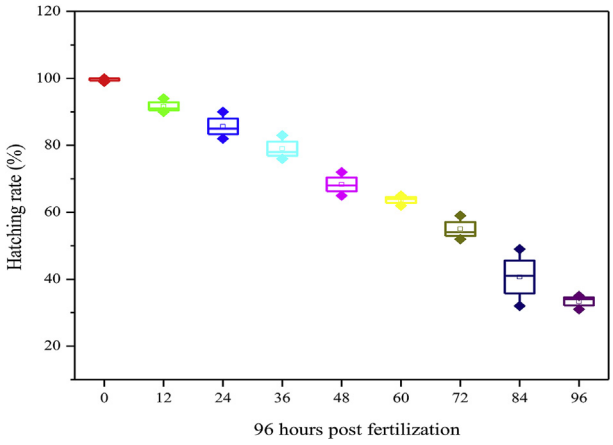

Fig. 8. Hatching percentage by fish study.

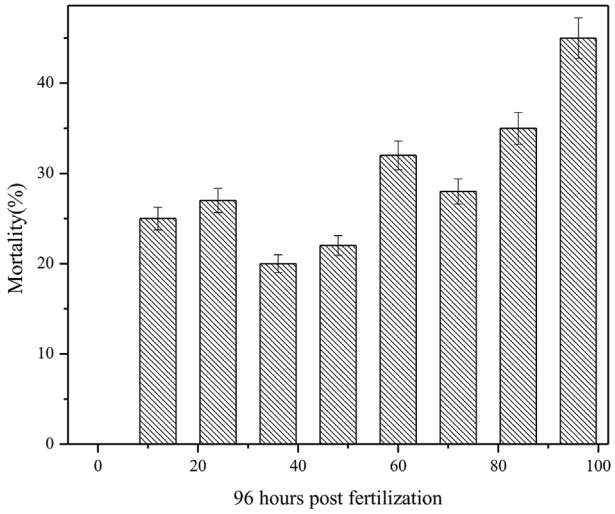

Fig. 9. Mortality rate.

which excludes external stabilizers or reducing agents and they are beneficial as an antimycotic agent. In future, the green synthesized silver nanoparticles will produce a large amount by the shampoo industries for the control of dermatophytes a major hair problem to the human beings and less toxic silver nanoparticles. Our results demonstrate silver nanoparticles disorders the standard organogenesis throughout development, and more elaborated studies are required to confirm silver nanoparticles with leaf extract unit of measurement toxicity management to be utilized in zebrafish.

Acknowledgements

The authors acknowledge Vellore Institute of Technology, School of Biosciences and Technology and Saveetha Dental College and Hospitals, Saveetha University for supporting this research.

References

Abourashed, E.A., Vanderplank, J.R., Khan, I.A., 2002. High-speed extraction and HPLC fingerprinting of medicinal plants – I. Application to Passiflora flavonoids. Pharm. Biol. 40, 81–91. https://doi.org/10.1076/phbi.40.2.81.5844.

Abourashed, E.A., Vanderplank, J., Khan, I. a., 2003. High-speed extraction and HPLC fingerprinting of medicinal plants – II. Application to harman alkaloids of genus Passiflora. Pharm. Biol. 41, 100–106. https://doi.org/10.1076/phbi.41.2.100.14244.

Abramenko, N.B., Demidova, T.B., Abkhalimov, E.V., Ershov, B.G., Krysanov, E.Y., Kustov, L.M., 2018. Ecotoxicity of different-shaped silver nanoparticles: case of zebrafish embryos. J. Hazard Mater. 347, 89–94. https://doi.org/10.1016/j.jhazmat.2017.12.060.

Alahmad, A., Eleoui, M., Falah, A., Alghoraibi, I., 2013. Preparation of colloidal structural characterization silver nanoparticles and. Phys. Sci. Res. Int. 1, 89–96.

Ali, M.S., Anuradha, V., Yogananth, N., Krishnakumar, S., 2019. Heart and liver re-generation in zebrafish using silver nanoparticle synthesized from Turbinaria

conoides – in vivo. Biocatal. Agric. Biotechnol. 17, 104–109. https://doi.org/10.1016/j.bcab.2018.10.013.
Amichai, B., Grunwald, M.H., 1998. Adverse drug reactions of the new oral antifungal agents - terbinafine, fluconazole, and itraconazole. Int. J. Dermatol. 37, 410–415. https://doi.org/10.1046/j.1365-4362.1998.00496.x.
Bar-Ilan, O., Albrecht, R.M., Fako, V.E., Furgeson, D.Y., 2009. Toxicity assessments of multisized gold and silver nanoparticles in zebrafish embryos. Small 5, 1897–1910. https://doi.org/10.1002/smll.200801716.
Berger, T.J., Spadaro, J.A., Chapin, S.E., Becker, R.O., 1976. Electrically generated silver ions: quantitative effects on bacterial and mammalian cells. Antimicrob. Agents Chemother. 9, 357–358. https://doi.org/10.1128/AAC.9.2.357.
Bhalodia, N., Shukla, V., 2011. Antibacterial and antifungal activities from leaf extracts of Cassia fistula l.: an ethnomedicinal plant. J. Adv. Pharm. Technol. Res. 2, 104. https://doi.org/10.4103/2231-4040.82956.
Dipankar, C., Murugan, S., 2012. The green synthesis, characterization and evaluation of the biological activities of silver nanoparticles synthesized from Iresine herbstii leaf aqueous extracts. Colloids Surfaces B Biointerfaces 98, 112–119. https://doi.org/10.1016/j.colsurfb.2012.04.006.
Govindarajan, M., Rajeswary, M., Veerakumar, K., Muthukumaran, U., Hoti, S.L., Benelli, G., 2016. Green synthesis and characterization of silver nanoparticles fabricated using Anisomeles indica: mosquitocidal potential against malaria, dengue and Japanese encephalitis vectors. Exp. Parasitol. 161, 40–47. https://doi.org/10.1016/j.exppara.2015.12.011.
Guidelines, O., The, F.O.R., Of, T., 2013. Test No. 236: fish embryo acute toxicity (FET) test 1–22. https://doi.org/10.1787/9789264203709-en.
K, A., J, V., 2017. Green synthesis and characterization of silver nanoparticles using vitex negundo (karu nochchi) leaf extract and its antibacterial activity. Med. Chem. 07, 218–225. https://doi.org/10.4172/2161-0444.1000460.
Kaba, S.I., Egorova, E.M., 2015. In vitro studies of the toxic effects of silver nanoparticles on HeLa and U937 cells. Nanotechnol. Sci. Appl. 8, 19–29. https://doi.org/10.2147/NSA.S78134.
Kanmani, P., Lim, S.T., 2013. Synthesis and characterization of pullulan-mediated silver nanoparticles and its antimicrobial activities. Carbohydr. Polym. 97, 421–428. https://doi.org/10.1016/j.carbpol.2013.04.048.
Kim, S.W., Jung, J.H., Lamsal, K., Kim, Y.S., Min, J.S., Lee, Y.S., 2012. Antifungal effects of silver nanoparticles (AgNPs) against various plant pathogenic fungi. MYCOBIOLOGY 40, 53–58. https://doi.org/10.5941/MYCO.2012.40.1.053.
Klaus-Joerger, T., Joerger, R., Olsson, E., Granqvist, C.G., 2001. Bacteria as workers in the living factory: metal-accumulating bacteria and their potential for materials science. Trends Biotechnol. 19, 15–20. https://doi.org/10.1016/S0167-7799(00)01514-6.
Krishnamurthy, S., Muthuswamy, S., Yun, Y.-S., 2009. Plant extract assisted reduction of platinum ions to nanoparticles. J. Biosci. Bioeng. 108, S91–S92. https://doi.org/10.1016/j.jbiosc.2009.08.269.
M. Awwad, A., M. Salem, N., O. Abdeen, A., 2013. Biosynthesis of silver nanoparticles using *Olea europaea* leaves extract and its antibacterial activity. Nanosci. Nanotechnol. 2, 164–170. https://doi.org/10.5923/j.nn.20120206.03.
Magudapathy, P., Gangopadhyay, P., Panigrahi, B.K., Nair, K.G.M., Dhara, S., 2001. Electrical transport studies of Ag nanoclusters embedded in glass matrix. Phys. B Condens. Matter 299, 142–146. https://doi.org/10.1016/S0921-4526(00)00580-9.
Mittal, A.K., Chisti, Y., Banerjee, U.C., 2013. Synthesis of metallic nanoparticles using plant extracts. Biotechnol. Adv. 31, 346–356. https://doi.org/10.1016/j.biotechadv.2013.01.003.
Mohanta, Y.K., Behera, S.K., 2014. Biosynthesis, characterization and antimicrobial activity of silver nanoparticles by Streptomyces sp. SS2. Bioprocess Biosyst. Eng. 37, 2263–2269. https://doi.org/10.1007/s00449-014-1205-6.
Mohanta, Y.K., Panda, S.K., Biswas, K., Tamang, A., Bandyopadhyay, J., De, D., Mohanta, D., Bastia, A.K., 2016. Biogenic synthesis of silver nanoparticles from Cassia fistula (Linn.): in vitro assessment of their antioxidant, antimicrobial and cytotoxic activities. IET Nanobiotechnol. 10, 438–444. https://doi.org/10.1049/iet-nbt.2015.0104.
Mosselhy, D.A., He, W., Li, D., Meng, Y., Feng, Q., 2016. Silver nanoparticles: in vivo toxicity in zebrafish embryos and a comparison to silver nitrate. J. Nanoparticle Res. 18, 1–15. https://doi.org/10.1007/s11051-016-3514-y.
Mousavi, S.A.A., Salari, S., Hadizadeh, S., 2015. Evaluation of antifungal effect of silver nanoparticles against Microsporum canis, Trichophyton mentagrophytes and Microsporum gypseum. Iran. J. Biotechnol. 13, 38–42. https://doi.org/10.15171/ijb.1302.
Nayak, D., Pradhan, S., Ashe, S., Rauta, P.R., Nayak, B., 2015. Biologically synthesised silver nanoparticles from three diverse family of plant extracts and their anticancer activity against epidermoid A431 carcinoma. J. Colloid Interface Sci. 457, 329–338. https://doi.org/10.1016/j.jcis.2015.07.012.
Rajeshkumar, S., Kayalvizhi, D., 2015. Antioxidant and hepatoprotective effect of aqueous and ethanolic extracts of important medicinal plant Pongamia pinnata (Family: Leguminoseae). Asian J. Pharmaceut. Clin. Res. 8, 67–70.
Rajeshkumar, S., Nagalingam, M., Ponnanikajamideen, M., Vanaja, M., Malarkodi, C., 2015. Anticancer activity of andrographis paniculata leaves extract against neuroblastima (Imr-32) and human colon (ht-29) cancer cell line. World J. Pharm. Pharmaceut. Sci. 4, 1667–1675.
Santhoshkumar, J., Kumar, S.V., Rajeshkumar, S., 2017. Synthesis of zinc oxide nanoparticles using plant leaf extract against urinary tract infection pathogen. Resour. Technol. 3, 459–465. https://doi.org/10.1016/j.reffit.2017.05.001.
Sarkar, B., Verma, S.K., Akhtar, J., Netam, S.P., Gupta, S.K., Panda, P.K., Mukherjee, K., 2018. Molecular aspect of silver nanoparticles regulated embryonic development in Zebrafish (Danio rerio) by Oct-4 expression. Chemosphere 206, 560–567. https://doi.org/10.1016/j.chemosphere.2018.05.018.
Singh, P.S., Vidyasagar, G.M., 2014. Activity of silver nanoparticles using raamphal plant (annona reticulata) aqueous leaves extract. Indian J. Mater. Sci. 2014, 5. https://doi.org/10.1155/2014/412452.
Syed, A., Ahmad, A., 2012. Extracellular biosynthesis of platinum nanoparticles using the fungus Fusarium oxysporum. Colloids Surfaces B Biointerfaces 97, 27–31. https://doi.org/10.1016/j.colsurfb.2012.03.026.
Van Aerle, R., Lange, A., Moorhouse, A., Paszkiewicz, K., Ball, K., Johnston, B.D., De-Bastos, E., Booth, T., Tyler, C.R., Santos, E.M., 2013. Molecular mechanisms of toxicity of silver nanoparticles in zebrafish embryos. Environ. Sci. Technol. 47, 8005–8014. https://doi.org/10.1021/es401758d.